

MIT Open Access Articles

Uptake Coefficients of Some Volatile Organic Compounds by Soot and Their Application in Understanding Particulate Matter Evolution in Aircraft Engine Exhaust Plumes

The MIT Faculty has made this article openly available. **Please share** how this access benefits you. Your story matters.

Citation: Yu, Zhenhong et al. "Uptake Coefficients of Some Volatile Organic Compounds by Soot and Their Application in Understanding Particulate Matter Evolution in Aircraft Engine Exhaust Plumes." *Journal of Engineering for Gas Turbines and Power* 136, 12 (June 27, 2014): 121501 © 2014 ASME

As Published: <http://dx.doi.org/10.1115/1.4027707>

Publisher: American Society of Mechanical Engineers (ASME)

Persistent URL: <http://hdl.handle.net/1721.1/114710>

Version: Final published version: final published article, as it appeared in a journal, conference proceedings, or other formally published context

Terms of Use: Article is made available in accordance with the publisher's policy and may be subject to US copyright law. Please refer to the publisher's site for terms of use.



Zhenhong Yu¹

Aerodyne Research, Inc.,
45 Manning Road,
BillERICA, MA 01821
e-mail: zyu@aerodyne.com

David S. Liscinsky

United Technologies Research Center,
411 Silver Lane,
East Hartford, CT 06108
e-mail: LiscinDS@utrc.utc.com

Bruce True

United Technologies Research Center,
411 Silver Lane,
East Hartford, CT 06108
e-mail: TrueBS@utrc.utc.com

Jay Peck

Aerodyne Research, Inc.,
45 Manning Road,
BillERICA, MA 01821
e-mail: jpeck@aerodyne.com

Archer C. Jennings

United Technologies Research Center,
411 Silver Lane,
East Hartford, CT 06108
e-mail: jenninac@utrc.utc.com

Hsi-Wu Wong

Aerodyne Research, Inc.,
45 Manning Road,
BillERICA, MA 01821
e-mail: hwwong@aerodyne.com

Mina Jun

Massachusetts Institute of Technology,
77 Massachusetts Avenue,
Cambridge, MA 02139
e-mail: mina.jun@gmail.com

Jonathan Franklin

Aerodyne Research, Inc.,
45 Manning Road,
BillERICA, MA 01821
e-mail: jfranklin@aerodyne.com

Scott C. Herndon

Aerodyne Research, Inc.,
45 Manning Road,
BillERICA, MA 01821
e-mail: herndon@aerodyne.com

Ian A. Waitz

Massachusetts Institute of Technology,
77 Massachusetts Avenue,
Cambridge, MA 02139
e-mail: iaw@mit.edu

Richard C. Miake-Lye

Aerodyne Research, Inc.,
45 Manning Road,
BillERICA, MA 01821
e-mail: rick@aerodyne.com

Uptake Coefficients of Some Volatile Organic Compounds by Soot and Their Application in Understanding Particulate Matter Evolution in Aircraft Engine Exhaust Plumes

To assist microphysical modeling on particulate matter (PM) evolution emitted from aircraft engines, uptake coefficients of some volatile organic compounds on soot were experimentally determined in this study. The determined values vary from $(1.0 \pm 0.1) \times 10^{-6}$ for water-miscible propylene glycol to $(2.5 \pm 0.1) \times 10^{-5}$ for 2,6-dimethylnaphthalene, a polycyclic aromatic hydrocarbon. An inverse power-law correlation between uptake coefficient on soot and solubility in water was observed. Using the correlation, microphysical simulations were performed for the exhaust plume evolution from an idling aircraft, and we found that the model-predicted volatile PM composition on soot is comparable with those results from past field measurements. [DOI: 10.1115/1.4027707]

¹Corresponding author.

Contributed by the Combustion and Fuels Committee of ASME for publication in the JOURNAL OF ENGINEERING FOR GAS TURBINES AND POWER. Manuscript received March 25, 2014; final manuscript received April 7, 2014; published online June 27, 2014. Editor: David Wisler.

1 Introduction

Particulate matter (PM) emissions from aircraft engines can have significant environmental impacts [1–6]. Both volatile and nonvolatile PMs are present in the exhaust of aircraft gas turbine engines. Emitted to the ambient air, the engine exhaust is diluted and cooled by the surrounding environment, so partitioning of the volatile species such as volatile organic compounds (VOCs) and sulfuric acid from gas-phase to PM starts after the engine exit plane. This process will continue via microphysical interactions over a distance of hundreds of meters downstream. Accurate quantification for both the nonvolatile black carbon soot emissions and the volatile contributions to particle mass is necessary for estimates of environmental and health impacts. The scientific understanding of volatile particle formation and growth for aircraft engine exhaust is still evolving, and neither a complete predictive capability nor a standard measurement approach has been developed. Investigations with microphysical plume models have demonstrated that aircraft soot emissions play an important role in contrail formation [7,8]. For the models to be quantitatively accurate, some critical parameters such as mass accommodation coefficients need to be determined experimentally for each interacting volatile species.

This experimental investigation quantifies specific VOC uptake on nonvolatile black carbon soot particles. A large number of uptake coefficient measurements have been made for several oxygenated compounds (e.g., HNO_3 , N_2O_5 , NO_x , and O_3) [9–25]. However this process has not been studied for VOCs present in the aircraft engine exhaust plume. For example, Saathoff et al. examined the coating of ozonolysis products of α -pinene on soot at a high relative humidity (RH \sim 90%) and found that the organic coating of soot particles leads to a compaction of the soot fractal agglomerates [26].

On the other hand, uptake of organic gas-phase species by ethylene glycol, 1-octanol, and 1-methylnaphthalene droplets has been extensively investigated by Zhang et al. [27,28]. They found that uptake coefficients of water-soluble species such as HCl by 1-methylnaphthalene is less than 10^{-3} compared to 0.44 and 0.47 for *m*-xylene and α -pinene, respectively. It appears that the chemical affinity of the interface and the physical properties of organic compounds play significant roles in uptake kinetics.

In a previous study [29], we demonstrated the determination of the uptake coefficient of naphthalene by simultaneously measuring the organic concentration in both the gas and PM phase. In this study, a number of polycyclic aromatic hydrocarbons (PAHs), including 1-methylnaphthalene ($\text{C}_{11}\text{H}_{10}$) and 2,6-dimethylnaphthalene ($\text{C}_{12}\text{H}_{12}$) were investigated for their uptake on combustion soot via a similar experimental setup. The solubility of 1-methylnaphthalene in water is 26 mg l^{-1} at ambient conditions while that of 2,6-dimethylnaphthalene is 1.3 mg l^{-1} [30]. Like the rest of PAHs, they are essentially water-insoluble and considered hydrophobic. In addition to 1-methylnaphthalene and 2,6-dimethylnaphthalene, three water-soluble volatile organic compounds were also investigated for their uptake properties. These compounds include two water-soluble organic alcohols, propylene glycol ($\text{C}_3\text{H}_8\text{O}_2$) and phenol ($\text{C}_6\text{H}_6\text{O}$), and one slightly water-soluble ($\sim 1 \text{ g/l}$) organic alcohol, 1-nonanol ($\text{C}_9\text{H}_{20}\text{O}$).

Among the studied organic compounds, phenol, methylnaphthalene, and dimethylnaphthalene have been detected by proton transfer reaction mass spectrometer in real-time from commercial aircraft engine exhausts in the past field investigations [31,32]. Phenol also belongs to the list of hazardous air pollutants in Sec. 112 of the U.S. Clean Air Act (1990). Since aircraft engines emit higher VOC levels at ground idle, our study will focus on uptake events at 293 K. The VOC levels applied in this study are comparable to the measured values from aircraft engine exhausts at ground idle.

The objective of this research project is to understand, quantify, and predict volatile particle evolution in aircraft-emitted plumes. Particles directly emitted from aircraft engines and generated

subsequently in the downstream plumes have significant impacts on climate, human health, and air quality. As a result of being cooled and diluted with ambient air, the properties and sizes of the PMs are drastically changed through microphysical processes within a residence time of a few minutes. To understand the impacts of aircraft-emitted PMs as well as to possibly formulate strategies to mitigate these impacts, it is important to understand the microphysical processes and the atmospheric evolution of PMs.

2 Experimental

The experimental system has been described in detail previously [29]. In brief, the system includes soot formation and sampling apparatus, a thermal soot denuder, vapor generation and mixing devices, and gas and particle detection instruments. Combustion soot particles were generated by a mini-CAST combustion aerosol standard (Jing Ltd., model 5200), which consists of a well-controlled propane diffusion flame. This soot generator has been applied as a reliable soot source in a number of investigations on combustion soot particles [33]. Although previous studies have found that uptake on soot varies with soot sources and fuels, it would be extremely difficult for us to directly use an aviation soot source for this study due to operational cost and safety. The mini-CAST is currently accepted as the standard soot source for instrument calibration during the demonstrations for an aerospace recommended practice on aviation soot measurements [34].

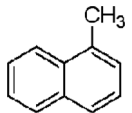
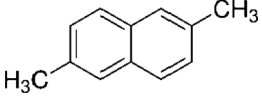

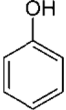
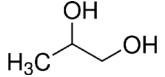
In this study, before mixing with the gaseous VOC to be studied, the soot stream was passed through a thermal soot denuder (Aerodyne Research, Inc.) operated at 150°C to remove the volatile composition and to ensure little organic coating on the soot particles. Previous field measurements on aircraft PM emissions revealed that volatile composition on aviation soot particles is relatively low at the engine exit plane [35]. Processing with the thermal denuder makes the mini-CAST-generated soot particle composition similar to aviation soot.

Particle size distribution in mobility diameter (D_m) was measured by a scanning mobility particle sizer (SMPS, model 3936, TSI), which consists of a differential mobility analyzer (model 3080, TSI) and a condensation particle counter (CPC, model 3025A, TSI). Black carbon mass of the soot particles was measured by a multiangle absorption photometer (MAAP, model 5012, Thermo Scientific). The gaseous VOC concentration was continuously monitored with a heated flame ionization detector (HFID, model 600, California Instruments) at 160°C [36], while the mass of VOC coatings on soot particles was measured by a compact time-of-flight aerosol mass spectrometer (CToF-AMS), manufactured by Aerodyne Research, Inc. [37–39]. The CToF-AMS is capable of simultaneously providing quantitative size and chemical mass loading information for nonrefractory nanoparticles. Since chemical composition of the particles are detected with the CToF-AMS by being heated on a roughened molybdenum surface under high vacuum (10^{-7} Torr) at about 600°C , it only detects the volatile and semivolatile composition of combustion soot particles. In principle, completely denuded soot particles cannot be monitored by this technique, while the coated soot particles are detectable. Characterization of the soot particles was reported in the previous study, and particle size and total number concentration of the soot were kept similar to the prior study of naphthalene [29].

At ambient conditions, all the species yield an appreciable vapor pressure (VP) from 2.8 Pa for 2,6-dimethylnaphthalene to 61 Pa for phenol, compared to less than 0.1 Pa for sulfuric acid. Using sulfuric acid as criteria reference suggests that all the applied VOCs are more volatile than sulfuric acid. All the studied VOCs are listed in Table 1 along with several important physical properties including melting point (MP), boiling point (BP), and VP at 25°C [40].

In this study, concentrations of the tested volatile species were controlled via a nitrogen flow over high-purity samples. Because of the relatively low vapor pressures of 2,6-dimethylnaphthalene

Table 1 List of VOC physical properties and uptake coefficients on combustion soot particles determined in this work

Name	Structural representation	MP (°C)	BP (°C)	VP at 25 °C (Pa)	γ	Solubility in water (g/l) ^a
1-methylnaphthalene		-22	240	9.03	$(1.16 \pm 0.6) \times 10^{-5}$	0.026
2,6-dimethylnaphthalene		106	264	2.12	$(2.5 \pm 0.1) \times 10^{-5}$	0.0013
1-nonanol		-6	214	3.03	$(3.3 \pm 0.7) \times 10^{-6}$	1.0
Phenol		43	182	46.6	$(1.9 \pm 0.1) \times 10^{-6}$	8.3
Propylene glycol		-59	188	20.0	$(1.0 \pm 0.1) \times 10^{-6}$	Fully miscible

^aFrom *Handbook of Aqueous Solubility Data*, 2nd ed., CRC Press, Boca Raton, FL.

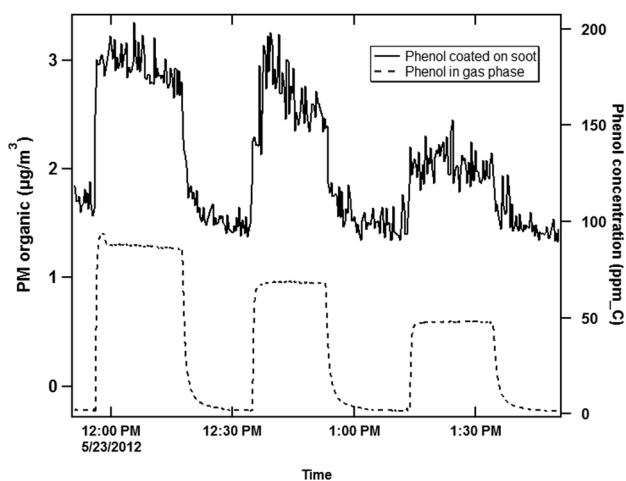


Fig. 1 A portion of simultaneous HFID and CTOf-AMS measurements on uptake of phenol by soot

(2.8 Pa) and 1-nonanol (4.0 Pa) at room temperature, the sampling tube was slightly heated to keep the temperature of 5–10 °C above room temperature for these two compounds in order to generate a well-detectable vapor for the HFID measurements. For all the studied compounds, vapor pressures of the mixed soot/VOC flow were below the species saturation limit so the gaseous compounds would not condense on the soot particles. The uptake of such volatile species only leads to a thin coating on the soot particles.

A portion of the simultaneous CTOf-AMS and HFID measurements on phenol is shown in Fig. 1. The green line is the measured total PM organic mass from the CTOf-AMS corrected for transmission efficiency [41] and the red line is the measured phenol concentration in the mixed soot/VOC flow by the HFID. The obtained PM organic mass responded almost simultaneously to the variation of phenol concentration, indicating that any response delay due to the large wall area of the sampling tube is negligible in this case. Experimental uncertainty is approximately $0.3 \mu\text{g m}^{-3}$ for the CTOf-AMS measurement and 0.1 ppm carbon for the HFID measurement. In this study, nitrogen carrier flow over the phenol sample was mixed with the soot flow to generate a test point for a period of approximately 30 min and then bypassed the phenol sample to yield a baseline period for the PM organic measurement from the CTOf-AMS. The obtained baseline

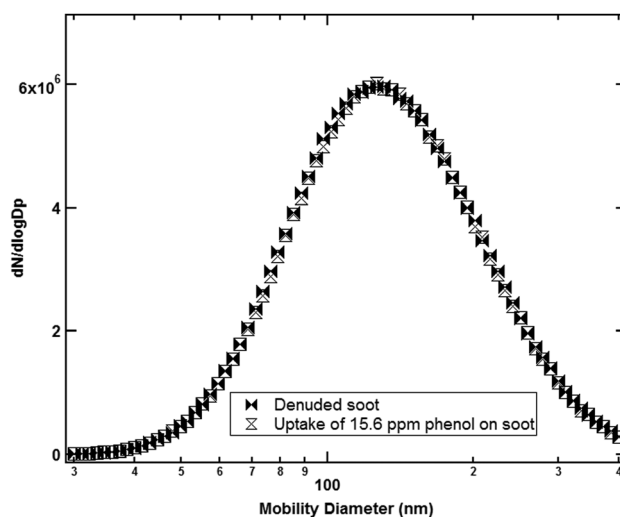


Fig. 2 The SMPS measurement on soot particle growth from uptake of 15.6 ppm phenol

represents the residue of volatile composition of soot particles after the thermal soot denuder.

3 Results and Discussions

3.1 Particle Size Growth. Since the vapor pressures of the mixed soot/VOC flow for all the studied VOCs were below their saturation limit, significant particle size growth from condensation on soot surface was not observed in this study. As shown in Fig. 2 from the SMPS measurement, the particle size distribution of the soot particles in mobility diameter (D_m) remains the same, with the geometric mean diameter equal to 121 ± 2 nm, after 15.6 ppm of phenol vapor was flowed with the denuded soot particles. We observed the same phenomenon for all the studied VOCs.

Our observation of little particle size growth from the SMPS measurement agrees with the CTOf-AMS and MAAP measurements on PM volatile and nonvolatile mass. For instance, with 15.6 ppm of phenol in the sample flow, PM organic mass concentration measured by the CTOf-AMS increases by $1.2 \mu\text{g/m}^3$, compared to the soot mass concentration of nearly 5 mg/m^3 measured by the MAAP. The small mass increase ($\sim 0.02\%$ compared to

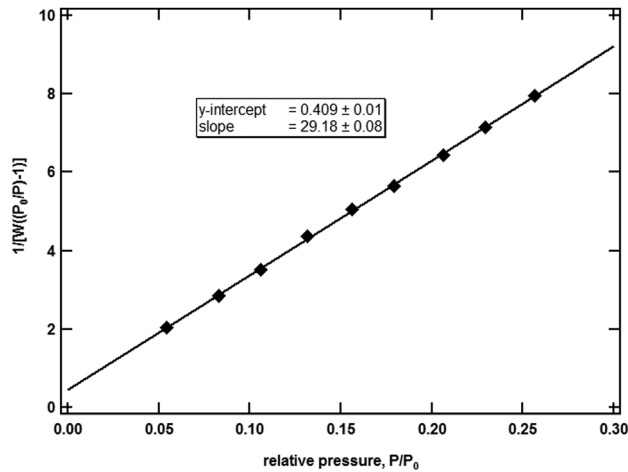


Fig. 3 The BET adsorption isotherm of the denuded combustion soot particles from mini-CAST soot generator

soot mass) due to the VOC coating on the soot surface does not create any detectable particle size growth.

According to analysis of uptake processes by Seinfeld and Pandis [42], there are three contributions to overall resistance to uptake: Gas-phase diffusion, mass accommodation at the surface, and interfacial transport/aqueous-phase diffusion. Given that the mass increase from the VOC coating on the soot surface is small, we believe that contribution from interfacial/transport/aqueous-phase diffusion is negligible in this study. In Sec. 3.2, we will also demonstrate that gas-phase diffusion resistance is very small compared to that from mass accommodation, so at first order approximation, the determined uptake coefficients can be considered as mass accommodation coefficients, which are critical for the microphysical model of PM evolution.

3.2 Determination of Uptake Coefficient. The methodology used to determine uptake coefficient for the investigated VOCs was the same as we described in the previous publication [29]. In brief, according to the kinetic uptake model developed by Worsnop and coworkers [43,44], the uptake coefficient, γ , defined as the probability of a gaseous VOC molecule sticking on the soot surface, can be determined as the following:

$$\frac{\Delta n}{n} = \gamma \frac{c A_d N}{4 F_g} \quad (1)$$

where Δn is the mass concentration of VOC coated on soot particles as measured by the CToF-AMS, n is the mass concentration of the VOC vapor measured by the HFID, c is the mean thermal velocity of VOC, which equals to $\sqrt{8RT/\pi M}$, N is the total number of soot particles determined from the SMPS measurement, A_d is the surface area of soot particle, and F_g is the volumetric flow rate.

In the previous study on naphthalene, the determination of A_d was based on the SMPS-AMS measurements [45,46]. Since combustion soot are fractal particles, determination of soot surface area with the SMPS-AMS method may result in a large uncertainty. To be more precise in quantification of surface area, we applied the Brunauer–Emmett–Teller (BET) method for nitrogen adsorption at liquid nitrogen temperature to determine surface area of the combustion soot [47,48]. The obtained BET adsorption isotherm for the mini-CAST-generated soot particles is plotted in Fig. 3, which yields the specific surface area of $118 \pm 4 \text{ m}^2 \text{ g}^{-1}$. Since particle count and mass in the sample flow was also simultaneously monitored by the CPC and MAAP, we thus obtained the average particle number per gram of soot, $C_d = (1.3 \pm 0.1) \times 10^{15} \text{ particle g}^{-1}$. Thus, A_d was determined to be $(9.1 \pm 0.7) \times 10^4 \text{ nm}^2$,

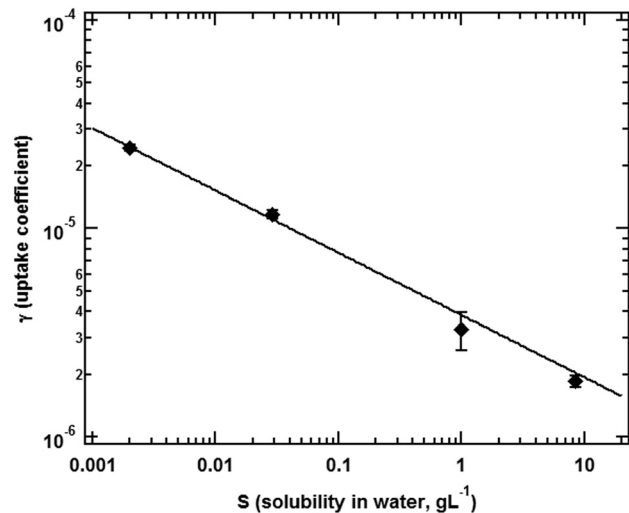


Fig. 4 The power-law correlation between γ and S , where γ is the determined uptake coefficient on soot and S is solubility in water. The linear regression fit yields $a = -0.30 \pm 0.02$ and constant $C = -5.41 \pm 0.02$, with a correlation coefficient, $R^2 = 0.998$, implying a very strong correlation.

by taking the ratio of the BET specific surface area to C_d . This result shows that the BET isotherm determined surface area is much larger than the geometric surface area, in agreement with the previous investigation by Aubin and Abbatt [49].

According to Eq. (1), the linear regressions of Δn versus $c n A_d N / (4 F_g)$ through the origin for all the measured VOCs were performed using the experimentally determined parameters. The determined uptake coefficients from the linear fit with one standard deviation uncertainty are listed in Table 1. Uptake coefficients for the aromatic 1-methylnaphthalene and 2,6-dimethylnaphthalene are larger than the water-soluble alcohols.

As we mentioned in Sec. 3.1 that, there are two contributions to uptake process: Gas-phase diffusion and mass accommodation on surface, which can be expressed as [28]

$$\frac{1}{\gamma} = \frac{1}{\Gamma_{\text{diff}}} + \frac{1}{\alpha} \quad (2)$$

Here, Γ_{diff} represents the effect of gas-phase diffusive transport on uptake and α is mass accommodation coefficient. Using the Fuchs–Sutugin formulation, Γ_{diff} can be calculated as [50]

$$\frac{1}{\Gamma_{\text{diff}}} = \frac{0.75 + 0.283 \text{Kn}}{\text{Kn}(1 + \text{Kn})} \begin{pmatrix} a_{11} & a_{12} & a_{13} \\ a_{21} & a_{22} & a_{23} \\ a_{31} & a_{32} & a_{33} \end{pmatrix} \quad (3)$$

where Knudsen number, $\text{Kn} = 2\lambda/d_f$; $\lambda = 3D_g/c$ is gas-phase mean free path, d_f is the diameter of the soot particle (121 nm in this case), and D_g is the diffusion coefficient of the VOCs under the experimental condition. Given that D_g is between 0.08 and $0.11 \text{ cm}^2/\text{s}$ for the studied VOCs, we found $1/\Gamma_{\text{diff}}$ is about 0.2 in this study. Our experimental measurements demonstrate that $1/\gamma$ varies from 4×10^4 for 2,6-dimethylnaphthalene to 1×10^6 for propylene glycol. These results suggest that the effect of gas-phase diffusion on uptake is negligible and the determined uptake coefficients can be considered as mass accommodation coefficients for these VOCs.

3.3 Uptake Coefficient and Solubility in Water. To understand the thermodynamic behavior of a complex chemical system, solubility in water has been used as a quantitative molecular parameter to correlate with a variety of molecular properties,

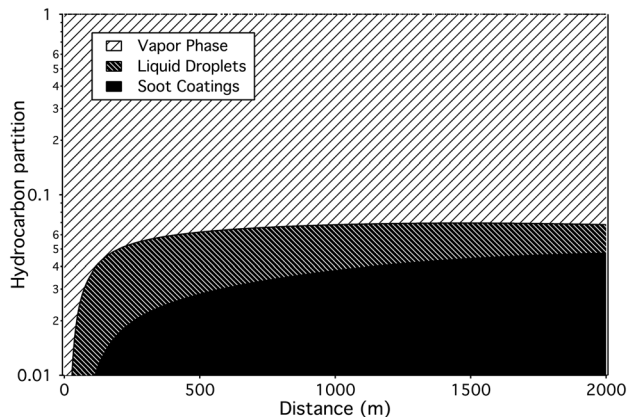


Fig. 5 The simulated mass fraction of naphthalene, methyl-naphthalene, dimethylnaphthalene, and phenol on soot emitted from CFM56 aircraft engine. The determined uptake coefficients in this study were used as dry mass accommodation coefficients in the modeling.

especially in the interpretation of hydrophobic interactions [51–56]. As shown in Table 1, propylene glycol, miscible in water, is the most water-soluble species among the group; while it has the smallest uptake coefficient, $\gamma = (1.0 \pm 0.1) \times 10^{-6}$. On the other hand, 2,6-dimethylnaphthalene is the least water-soluble (solubility in water = 0.0013 g l^{-1}) but its uptake coefficient, $\gamma = (2.5 \pm 0.1) \times 10^{-5}$, is the largest, about twenty times larger than propylene glycol. It appears that the obtained uptake coefficient values of the organic species investigated in this study inversely correlate with their solubility in water. Fresh combustion soot is typically considered as hydrophobic and this statement has been proved experimentally in the past through aging the soot particles [10,11]. For instance, Zuberi et al. oxidized fresh soot by exposure to OH and O_3 in the presence of UV radiation. They found that the mass due to water uptake on the aged soot increases with aging time [11]. Our experimental observation is consistent with the conventional thought that combustion soot particles are hydrophobic so water-insoluble hydrocarbons like PAH have larger uptake coefficient than the water-soluble species such as alcohols and organic acids.

To further quantify the observed correlation between uptake coefficient and solubility in water, we presented this inverse correlation in a logarithm plot, as shown in Fig. 4. The logarithm of uptake coefficients varies in a linearly inverse correlation with the logarithm of solubility in water, in g l^{-1} , as the following:

$$\log \gamma = a \log S_{\text{aq}} + C \quad (4)$$

where S_{aq} is the solubility in water. The slope of this linear fit in Fig. 5 is determined to be $a = -0.30 \pm 0.02$, with a correlation coefficient, R , value of 0.999, implying a very strong correlation. The value for constant C from the fitting is -5.41 ± 0.02 . This plot suggests that a phenomenological power-law correlation exists between VOC uptake coefficients on denuded combustion soot and solubility in water.

As demonstrated in this study and other investigations [29] on uptake of organic compounds on soot surface, uptake coefficients of VOCs on soot are usually small. Thus, measuring uptake coefficient requires determination of VOC concentration in a large dynamic range, normally more than five orders of magnitude. This makes its experimental measurement difficult and expensive. Solubility in water is a well-known physical property for a large number of organic compounds. The correlation between uptake coefficient on soot and solubility in water may help to estimate the uptake properties without many costly experimental measurements.

3.4 VOC Partition in Aircraft Engine Exhaust. We have previously developed a microphysical simulation model to takes

complex vapor to liquid partitioning and plume dilution and mixing with ambient air into account. The model has been described in detail in the previous publications [57,58]. The model takes the engine exit state, including parameters about gaseous species composition as well as soot size and loading, and ambient cooling/dilution profile as the user inputs, and simulates how the species condense and form PMs by accounting for nucleation, coagulation, and soot coating. One of the major challenges to apply this model to obtain quantitative predictions is the lack of accurate VOC mass accommodation coefficients on soot surface. The results from this laboratory study on uptake coefficients of VOCs by combustion soot particles provide the valuable experimental measurements and also enable the use of relevant uptake coefficient values based on the known water solubility in the model. As we discussed in Secs. 3.1 and 3.2, the determined uptake coefficients can be considered as mass accommodation coefficients under the present experimental conditions.

Using the results from this study, we simulated the CFM56-2C1 engine studied in the aircraft particle emissions experiment (APEX) at idle (7%) power using our detailed microphysical model. Based on the gas-particle partitioning method proposed by Robinson and coworkers to represent the volatile organics distribution in diesel exhaust [59,60], our modeling study was performed with six organic compounds: Pentanoic acid ($\text{C}_5\text{H}_{10}\text{O}_2$), naphthalene (C_{10}H_8), anthracene ($\text{C}_{14}\text{H}_{10}$), pyrene ($\text{C}_{16}\text{H}_{10}$), perylene ($\text{C}_{20}\text{H}_{12}$), and anthanthrene ($\text{C}_{22}\text{H}_{12}$). The selected VOC species have ambient saturation vapor concentrations on the order of 10^6 , 10^4 , 10^2 , 10^0 , and $10^{-2} \mu\text{g m}^{-3}$, and the relative composition among the species was assumed to follow the half of a log-normal distribution with respect to the saturation vapor concentration. Low volatility organic species in engine emissions are usually water-insoluble, and thus, we selected one water-insoluble VOC for each volatility bin except for the highest volatility ($10^6 \mu\text{g m}^{-3}$), where one water-soluble and one water-insoluble were used. The sum of each VOC concentrations was set to 3.6 ppm, which would give a naphthalene concentration of 1 ppm that matches the value that was measured during APEX [6].

Sulfuric acid concentration at the engine exit was estimated based on 600 ppm fuel sulfur content and 0.35% conversion from SO_2 to sulfuric acid. The estimated conversion rate comes from previous theoretical and experimental investigations, which found that only a small portion of SO_2 was converted into sulfuric acid [61–65]. To reduce computation time, soot emissions at the engine exit plane were assumed to be monodisperse with a diameter of 20 nm and a concentration of $3.4 \times 10^8 \text{ cm}^{-3}$. The dilution and cooling profile was calculated by an empirical model by Nickels and Perry's turbulent coflowing jet [65,66] using an ambient temperature of 293 K and an ambient relative humidity of 60%. Microphysical evolution of soot particles up to 2 km downstream of the engine was specifically tracked.

As shown in Fig. 5, mass fractions of total organic compounds in nucleation particles on soot surface and in gas-phase were predicted as a function of downstream distance. Organic compounds in PM are initially predominant in the liquid droplets (nucleation mode particles). After the soot surface is activated by sulfuric acid, more organics are uptaken on soot. Due to the volatile nature of these organic compounds, their final mass fractions in PM is small (<7%) compared to those in the gas-phase. In contrast, as presented in Fig. 6, the mass fraction of sulfuric acid in PM increases from about 25% at 100 m to almost 100% at 1000 m, indicating significant partitioning from the gas-phase into the PM phase. This is not only because of sulfuric acid's large uptake coefficients but also due to its low saturation vapor pressure at room temperature. Because the VOCs have much higher initial gas-phase concentrations, however, the contribution from organics eventually becomes more significant than sulfuric acid as shown in Fig. 7.

In Fig. 7, the modeling results demonstrate that the soot particles emitted by an idling aircraft continue increase over a long distance. At the current condition, contribution from sulfuric acid

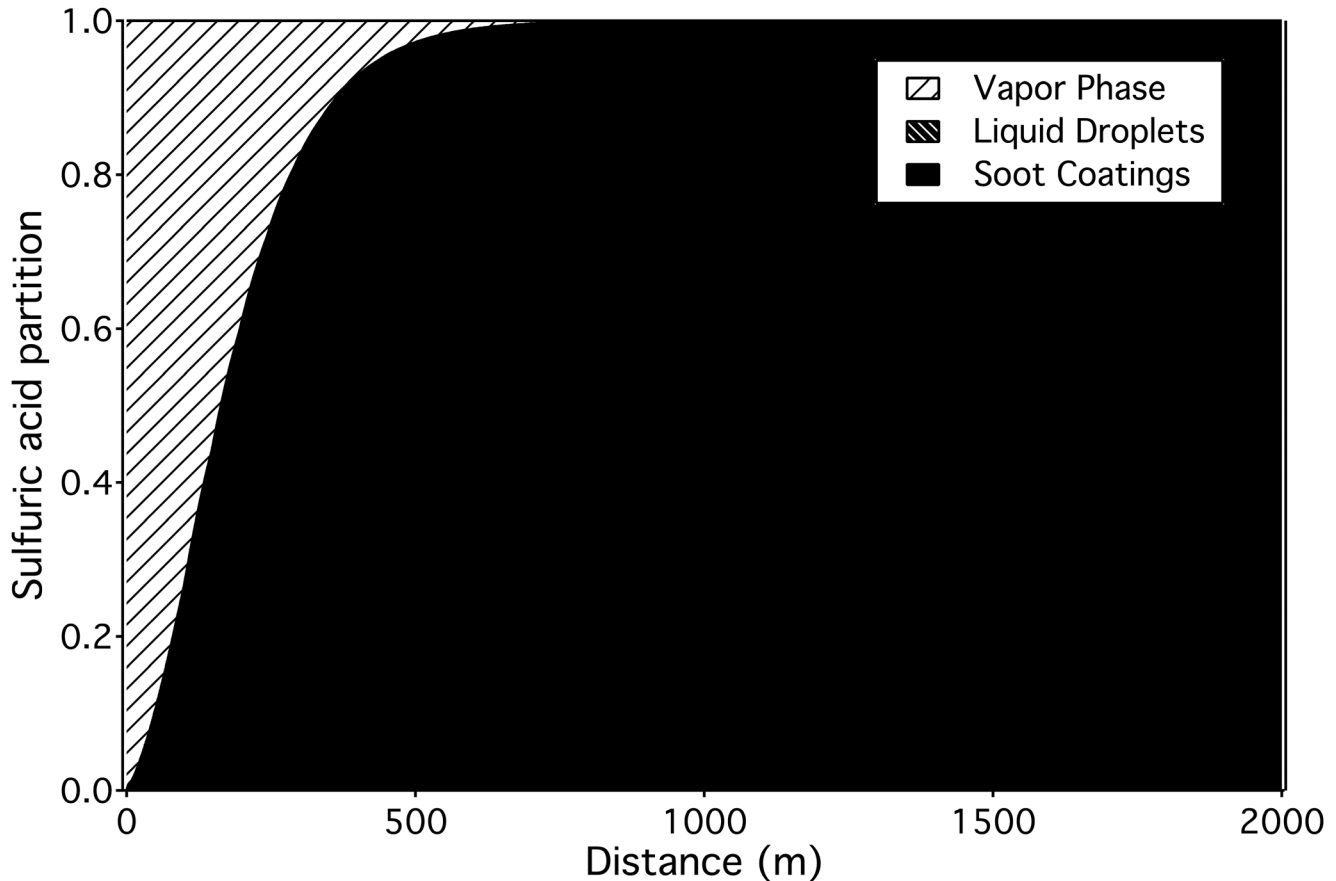


Fig. 6 The simulated mass fraction of sulfuric acid in vapor phase, liquid droplets, and coated on soot surface emitted from a CFM56 aircraft engine

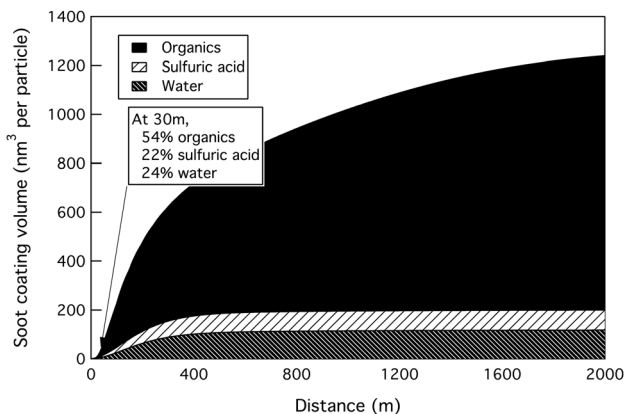


Fig. 7 Volume increase per particle versus downstream distance, due to volatile PM composition coated on soot surface, including organics, sulfuric acid and water

reaches a maximum around 500m downstream when almost 100% of sulfuric acid is coated on soot; while the contribution from organics keeps increasing further. The initial soot diameter increases from 20nm at the engine exit to about 21.5 at 1000m downstream via uptake of volatile species.

In comparison with the field measurements, our simulation results predict that at 30m downstream, volatile PM on soot surface contains 54% organic, 24% water, and 22% sulfate; while the previous AMS measurements from a 30m probe showed an averaged semivolatile PM composition of 56% organic and 44% sulfate for a number of CFM56 engines [35]. The result from the microphysical simulation is in a good agreement with the

experimental values, given that experimental uncertainties are normally large. Water detection by the AMS has been only qualitative because of its vaporization in vacuum. Going further downstream, the plume is highly diluted and influenced by the wind and other ambient activities, and it is difficult to quantify the volatile species with high confidence. However, our previous measurement experience is that the PM in the long-aged plume is usually dominated by organics, which is consistent with the simulation results.

The results from the microphysical modeling suggest that both uptake and volatility are critical in determining gas to particle partitioning on aviation soot particles. Thus, this laboratory study of VOC uptake coefficients on soot can be extended to those species that are semivolatile in nature, which are sensitive to uptake coefficients in the near-field and have low enough vapor pressure to have significant condensation further downstream. Given the complexity of volatile PM evolution in aircraft engine exhausts, although our modeling provides comparable results to the field measurements, precision of a number of critical parameters especially those that are temperature-dependent still needs to be verified.

4 Summary

We determined uptake coefficients of 1-methylnaphthalene, 2,6-dimethylnaphthalene, 1-nonanol, phenol, and propylene glycol on combustion soot particles in this study. Little condensational growth on soot particles was observed due to the subsaturated vapor pressure of these gas-phase species allowing the uptake process to be independently studied. An inverse power-law correlation between uptake coefficient of a VOC species on soot and solubility of the same species in water was found from our

measurements, suggesting that it is possible to predict uptake coefficients on soot via their correlation with solubility in water.

We performed a microphysical simulation using a 6-species PM surrogate model with mass accommodation coefficients based on this finding, and we found that almost 100% of sulfuric acid quickly coats on the soot particles within the first 500 m and, although slow, the organic compounds continues to condense and eventually dominate the soot coating composition. This modeling result agrees well with plume exhaust measurement data from tests on a CFM56-2C1 aircraft engine.

Acknowledgment

The authors would like to thank Dr. Meredith Colket at UTRC, Dr. Bruce Anderson and Dr. Richard Moore at NASA Langley Research Center for helpful discussions during the course of this work.

This study was financially supported by the Strategic Environmental Research and Development Program (SERDP) of Department of Defense Contract No. W912HQ-08-C-0052 (WP-1625).

Nomenclature

APEX	= aircraft particle emissions experiment
BET	= Brunauer–Emmett–Teller
CPC	= condensation particle counter
CToF-AMS	= compact time-of-flight aerosol mass spectrometer
D_m	= mobility diameter
GMD	= geometric mean diameter
HAP	= hazardous air pollutant
HFID	= heated flame ionization detector
MAAP	= multiangle absorption photometer
PAH	= polycyclic aromatic hydrocarbon
PM	= particulate matter
PTR-MS	= proton transfer reaction—mass spectrometer
RH	= relative humidity
SMPS	= scanning mobility particle sizer
VOC	= volatile organic compound

References

- [1] Schlager, H., Konopka, P., Schulte, P., Schumann, U., Ziereis, H., Arnold, F., Klemm, M., Hagen, D. E., Whitefield, P. D., and Ovarlez, J., 1997, "In Situ Observation of Air Traffic Emission Signatures in the North Atlantic Flight Corridor," *J. Geophys. Res.*, **102**(D9), pp. 10739–10750.
- [2] Anderson, B. E., Cofer, W. R., Bagwell, D. R., Barrick, J. W., Hudgins, C. H., and Brunke, K. E., 1998, "Airborne Observations of Aircraft Aerosol Emissions I: Total Nonvolatile Particle Emission Indices," *Geophys. Res. Lett.*, **25**(10), pp. 1689–1692.
- [3] Paladino, J., Whitefield, P., Hagen, D., Hopkins, A. R., and Trueblood, M., 1998, "Particle Concentration Characterization for Jet Engine Emissions Under Cruise Conditions," *Geophys. Res. Lett.*, **25**(10), pp. 1697–1700.
- [4] Schuman, U., Arnold, F., Busen, R., Curtis, J., Kärcher, B., Kiendler, A., Petzold, A., Schlager, H., Schroder, F., and Wohlfrom, K. H., 2002, "Influence of Fuel Sulfur on the Composition of Aircraft Exhaust Plumes: The Experiments SULFUR 1-7," *J. Geophys. Res.*, **107**(D15), p. 4247.
- [5] Unal, A., Hu, Y., Chang, M. E., Talat Odman, M., and Russell, A. G., 2005, "Airport Related Emissions and Impacts on Air Quality: Application to the Atlanta International Airport," *Atmos. Environ.*, **39**(32), pp. 5787–5798.
- [6] Wey, C. C., Anderson, B. E., Wey, C., Miake-Lye, R. C., Whitefield, P., and Howard, R., 2007, "Overview on the Aircraft Particle Emissions Experiment," *J. Propul. Power*, **23**(5), pp. 898–905.
- [7] Kärcher, B., and Yu, F., 2009, "Role of Aircraft Soot Emissions in Contrail Formation," *Geophys. Res. Lett.*, **36**(1), p. L01804.
- [8] Wong, H.-W., and Miake-Lye, R. C., 2010, "Parametric Studies of Contrail Ice Particle Formation in Jet Regime Using One-Dimensional Microphysical Modeling," *Atmos. Chem. Phys.*, **10**(7), pp. 3261–3272.
- [9] Seisel, S., Lian, Y., Keil, T., Trukhin, M. E., and Zellner, R., 2004, "Kinetics of the Interaction of Water Vapor With Mineral Dust and Soot Surfaces at $T = 298$ K," *Phys. Chem. Chem. Phys.*, **6**(8), pp. 1926–1932.
- [10] Kotzick, R., Panne, U., and Niessner, R., 1997, "Changes in Condensation Properties of Ultrafine Carbon Particles Subjected to Oxidation by Ozone," *J. Aerosol Sci.*, **28**(5), pp. 725–735.
- [11] Zuberi, B., Johnson, K. S., Aleks, G. K., Molina, L. T., Molina, M. J., and Laskin, A., 2005, "Hydrophilic Properties of Aged Soot," *Geophys. Res. Lett.*, **32**(1), p. L01807.
- [12] Prince, A. P., Wade, J. L., Grassian, V. H., Kleiber, P. D., and Yound, M. A., 2002, "Heterogeneous Reactions of Soot Aerosols With Nitrogen Dioxide and Nitric Acid: Atmospheric Chamber and Knudsen Cell Studies," *Atmos. Environ.*, **36**(36–37), pp. 5729–5740.
- [13] Zuberi, B., Jognson, K. S., Aleks, G. K., Molina, L. T., Molina, M. J., and Laskin, A., 2005, "Hydrophilic Properties of Aged Soot," *Geophys. Res. Lett.*, **32**(1), p. L01807.
- [14] Disselkamp, R. S., Carpenter, M. A., and Cowin, J. P., 2000, "A Chamber Investigation of Nitric Acid-Soot Aerosol Chemistry at 298 K," *J. Atmos. Chem.*, **37**(2), pp. 113–123.
- [15] Kleffmann, J., and Wiesen, P., 2005, "Heterogeneous Conversion of NO_2 and NO on HNO_3 Treated Soot Surfaces: Atmospheric Implications," *Atmos. Chem. Phys.*, **5**(1), pp. 77–83.
- [16] Longfellow, C. A., Ravishankara, A. R., and Hanson, D. R., 2000, "Reactive and Nonreactive Uptake on Hydrocarbon Soot: HNO_3 , O_3 , and N_2O_5 ," *J. Geophys. Res.*, **105**(D19), pp. 24345–24350.
- [17] Talukdar, R. K., Loukhovitskaya, E. E., Popovicheva, O. B., and Ravishankara, A. R., 2006, "Uptake of HNO_3 on Hexane and Aviation Kerosene Soots," *J. Phys. Chem. A*, **110**(31), pp. 9643–9653.
- [18] Rogaski, C. A., Golden, D. M., and Williams, L. R., 1997, "Reactive Uptake and Hydration Experiments on Amorphous Carbon Treated With NO_2 , SO_2 , O_3 , HNO_3 , and H_2SO_4 ," *Geophys. Res. Lett.*, **24**(4), pp. 381–384.
- [19] Saathoff, H., Naumann, K.-H., Riemer, N., Kamm, S., Möhler, O., Schurath, U., Vogel, H., and Vogel, B., 2001, "The Loss of NO_2 , HNO_3 , $\text{NO}_2/\text{N}_2\text{O}_5$, and $\text{HO}_2/\text{HOONO}_2$ on Soot Aerosol: A Chamber and Modeling Study," *Geophys. Res. Lett.*, **28**(10), pp. 1957–1960.
- [20] Kircher, U., Scheer, V., and Vogt, R., 2000, "FTIR Spectroscopic Investigation of the Mechanism and Kinetics of the Heterogeneous Reaction of NO_2 and HNO_3 With Soot," *J. Phys. Chem. A*, **104**(39), pp. 8908–8915.
- [21] Karagulian, F., and Rossi, M. J., 2007, "Heterogeneous Chemistry of the NO_3 Free Radical and N_2O_5 on Decane Flame Soot at Ambient Temperature: Reaction Products and Kinetics," *J. Phys. Chem. A*, **111**(10), pp. 1914–1926.
- [22] Rodriguez-Forata, A., and Iannuzzi, M., 2008, "First-Principles Molecular Dynamics Study of the Heterogeneous Reduction of NO_2 on Soot Surface," *J. Phys. Chem. C*, **112**(49), pp. 19642–19648.
- [23] Aubin, D. G., and Abbatt, J. P. D., 2007, "Interaction of NO_2 With Hydrocarbon Soot: Focus on HONO Yield, Surface Modification, and Mechanism," *J. Phys. Chem. A*, **111**(28), pp. 6263–6273.
- [24] Ghigo, G., Causa, M., Maranzana, A., and Tonachini, G., 2006, "Aromatic Hydrocarbon Nitration Under Tropospheric and Combustion Conditions. A Theoretical Mechanistic Study," *J. Phys. Chem. A*, **110**(49), pp. 13270–13282.
- [25] Ammann, M., Kalberer, M., Jost, D. T., Tobler, L., Rössler, E., Piguert, D., Gäggeler, H. W., and Baltensperger, U., 1998, "Heterogeneous Production of Nitrous Acid on Soot in Polluted Air Masses," *Nature*, **395**(6698), pp. 157–160.
- [26] Saathoff, H., Naumann, K.-H., Möhler, O., Jonsson, A. M., Hallquist, M., Kiendler-Scharr, A., Mentel, Th. F., Tillmann, R., and Schurath, U., 2008, "Temperature Dependence of Yields of Secondary Organic Aerosols From the Ozonolysis of α -Pinene and Limonene," *Atmos. Chem. Phys. Discuss.*, **8**(4), pp. 15595–15664.
- [27] Zhang, H. Z., Li, Y. Q., Xia, J. R., Davidovits, P., Williams, L. R., Jayne, J. T., Kolb, C. E., and Worsnop, D. R., 2003, "Uptake of Gas-Phase Species by 1-Octanol. I. Uptake of α -Pinene, γ -Terpinene, p -Cymene, and 2-Methyl-2-Hexanol as a Function of Relative Humidity and Temperature," *J. Phys. Chem. A*, **107**(33), pp. 6388–6397.
- [28] Zhang, H. Z., Li, Y. Q., Davidovits, P., Williams, L. R., Jayne, J. T., Kolb, C. E., and Worsnop, D. R., 2003, "Uptake of Gas-Phase Species by 1-Octanol. II. Uptake of Hydrogen Halides and Acetic Acid as a Function of Relative Humidity and Temperature," *J. Phys. Chem. A*, **107**(33), pp. 6398–6407.
- [29] Liscinsky, D. S., Yu, Z., True, B., Peck, J., Jennings, A. C., Wong, H. W., Jun, M., Franklin, J., Herndon, S. C., Waitz, I., and Miake-Lye, R. C., 2013, "Uptake of Naphthalene by Combustion Soot Particles," *Environ. Sci. Technol.*, **47**(9), pp. 4875–4881.
- [30] Eganhouse, R. P., and Calder, J. A., 1976, "The Solubility of Medium Molecular Weight Aromatic Hydrocarbons and the Effects of Hydrocarbon Co-Solutes and Salinity," *Geochim. Cosmochim. Acta*, **40**(5), pp. 555–561.
- [31] Spicer, C. W., Holdren, M. W., Smith, D. L., Hughes, D. P., and Smith, M. D., 1992, "Chemical Composition of Exhaust From Aircraft Turbine Engines," *ASME J. Eng. Gas Turbines Power*, **114**(1), pp. 111–117.
- [32] Knighton, W. B., Rogers, T., Wey, C. C., Anderson, B. E., Herndon, S. C., Yelvington, P. E., and Miake-Lye, R. C., 2007, "Application of Proton Transfer Reaction Mass Spectrometry (PTR-MS) for Measurement of Volatile Organic Trace Gas Emissions From Aircraft," *J. Propul. Power*, **23**(5), pp. 949–958.
- [33] Henning, S., Ziese, M., Kiselev, A., Saathoff, H., Möhler, O., Mentel, T. F., Buchholz, A., Spindler, C., Michaud, V., Monier, M., Sellegrri, K., and Stratmann, F., 2012, "Hygroscopic Growth and Droplet Activation of Soot Particles: Uncoated, Succinic or Sulfuric Acid Coated," *Atmos. Chem. Phys.*, **12**(10), pp. 4525–4537.
- [34] Marsh, R., Crayford, A., Petzold, A., Johnson, M., Williams, P., Ibrahim, A., Kay, P., Morris, S., Delhaye, D., Lottin, D., Vancassel, X., Raper, D., Christie, S., Bennett, M., Miller, M., Sevenco, Y., Rojo, C., Coe, H., and Bowen, P., 2011, "Studying, Sampling and Measuring of Aircraft Particulate Emissions II (SAMPLE II)—Final Report," European Aviation Safety Agency, Cologne, Germany, Report No. EASA.2009.OP.18.
- [35] Timko, M. T., Onasch, T. B., Northway, M. J., Jayne, J. T., Canagaratna, M. R., Herndon, S. C., Wood, E. C., Miake-Lye, R. C., and Knighton, W. B., 2010, "Gas Turbine Engine Emissions—Part II: Chemical Properties of Particulate Matter," *ASME J. Eng. Gas Turbine Power*, **132**(6), p. 061505.
- [36] McWilliam, I. G., and DeWar, R. A., 1958, "Flame Ionization Detector for Gas Chromatography," *Nature*, **181**(4611), p. 760.

- [37] Jayne, J. T., Leard, D. C., Zhang, X., Davidovits, P., Smith, K. A., Kolb, C. E., and Worsnop, D. R., 2000, "Development of an Aerosol Mass Spectrometer for Size and Composition Analysis of Submicron Particles," *Aerosol Sci. Technol.*, **33**(1-2), pp. 49–70.
- [38] Jimenez, J. L., Jayne, J. T., Shi, Q., Kolb, C. E., Worsnop, D. R., Yourshaw, I., Seinfeld, J. H., Flagan, R. C., Zhang, X., Smith, K. A., Morris, J., and Davidovits, P., 2003, "Ambient Aerosol Sampling Using the Aerodyne Aerosol Mass Spectrometer," *J. Geophys. Res.*, **108**(D7), p. 8425.
- [39] Canagaratna, M. R., Jayne, J. T., Jimenez, J. L., Allan, J. D., Alfarra, M. R., Zhang, Q., Onasch, T. B., Drewnick, F., Coe, H., Middlebrook, A., Delia, A., Williams, L. R., Trimborn, A. M., Northway, M. J., DeCarlo, P. F., Kolb, C. E., Davidovits, P., and Worsnop, D. R., 2007, "Chemical and Microphysical Characterization of Ambient Aerosols With the Aerodyne Aerosol Mass Spectrometer," *Mass Spectrosc. Rev.*, **26**(2), pp. 185–222.
- [40] Linstrom, P. J., and Mallard, W. J., eds., *NIST Chemistry WebBook, NIST Standard Reference Database Number 69*, National Institute of Standards and Technology, Gaithersburg, MD.
- [41] Liu, P. S. K., Deng, R., Smith, K. A., Williams, L. R., Jayne, J. T., Canagaratna, M. R., Moore, K., Onasch, T. B., Worsnop, D. R., and Deshler, T., 2007, "Transmission Efficiency of an Aerodynamic Focusing Lens System: Comparison of Model Calculations and Laboratory Measurements for the Aerodyne Aerosol Mass Spectrometer," *Aerosol Sci. Technol.*, **41**(8), pp. 721–733.
- [42] Seinfeld, J. H., and Pandis, S. N., 1998, *Atmospheric Chemistry and Physics: From Air Pollution to Climate Change*, Wiley, New York.
- [43] Davidovits, P., Hu, J. H., Worsnop, D. R., Zahniser, M. S., and Kolb, C. E., 1995, "Entry of Gas Molecules Into Liquids," *Faraday Discuss.*, **100**, pp. 65–82.
- [44] Worsnop, D. R., Zahniser, M. S., Kolb, C. E., Gardner, J. A., Watson, L. R., Van Doren, J. M., Jayne, J. T., and Davidovits, P., 1989, "Temperature Dependence of Mass Accommodation of SO₂ and H₂O₂ on Aqueous Surfaces," *J. Phys. Chem.*, **93**(3), pp. 1159–1172.
- [45] DeCarlo, P. F., Slowik, J. G., Worsnop, D. R., Davidovits, P., and Jimenez, J. L., 2004, "Particle Morphology and Density Characterization by Combined Mobility and Aerodynamic Diameter Measurements. Part 1: Theory," *Aerosol Sci. Technol.*, **38**(12), pp. 1185–1205.
- [46] Slowik, J. G., Stainken, K., Davidovits, P., Williams, L. R., Jayne, J. T., Kolb, C. E., Worsnop, D. R., Rudich, Y., DeCarlo, P. F., and Jimenez, J. L., 2004, "Particle Morphology and Density Characterization by Combined Mobility and Aerodynamic Diameter Measurements. Part 2: Application to Combustion-Generated Soot Aerosols as a Function of Fuel Equivalence Ratio," *Aerosol Sci. Technol.*, **38**(12), pp. 1206–1222.
- [47] Brunauer, S., Emmett, P. H., and Teller, E., 1938, "Adsorption of Gases in Multi-Molecular Layers," *J. Am. Chem. Soc.*, **60**(2), pp. 309–319.
- [48] Leviitt, N. P., Zhang, R., Xue, H., and Chen, J., 2007, "Heterogeneous Chemistry of Organic Acids on Soot Surfaces," *J. Phys. Chem. A*, **111**(22), pp. 4804–4814.
- [49] Aubin, D. G., and Abbott, J. P., 2003, "Adsorption of Gaseous Nitric Acid to n-Hexane Soot: Thermodynamics and Mechanism," *J. Phys. Chem. A*, **107**(50), pp. 11030–11037.
- [50] Hanson, D. R., Ravishankara, A. R., and Lovejoy, E. R., 1996, "Reaction of BrONO₂ With H₂O on Submicron Sulfuric Acid Aerosol and the Implications for the Lower Stratosphere," *J. Geophys. Res.*, **101**(D4), pp. 9063–9069.
- [51] Hermann, R. B., 1972, "Theory of Hydrophobic Bonding. II. Correlation of Hydrocarbon Solubility in Water With Solvent Cavity Surface Area," *J. Phys. Chem.*, **76**(19), pp. 2754–2759.
- [52] Pierotti, R. A., 1976, "A Scaled Particle Theory of Aqueous and Nonaqueous Solutions," *Chem. Rev.*, **76**(6), pp. 717–726.
- [53] Breslow, R., 1991, "Hydrophobic Effect on Simple Organic Reactions in Water," *Acc. Chem. Res.*, **24**(6), pp. 159–164.
- [54] Ruelle, P., Buchmann, M., Nam-Tran, H., and Kesselring, U. W., 1992, "Comparison of the Solubility of Polycyclic Aromatic Hydrocarbons in Non-associated and Associated Solvents: The Hydrophobic Effect," *Int. J. Pharm.*, **87**(1-3), pp. 47–57.
- [55] Seth, R., Mackay, D., and Muncke, J., 1999, "Estimating the Organic Carbon Partition Coefficient and Its Variability for Hydrophobic Chemicals," *Environ. Sci. Technol.*, **33**(14), pp. 2390–2394.
- [56] Meyer, E. E., Rosenberg, K. J., and Israelachvili, J., 2006, "Recent Progress in Understanding Hydrophobic Interactions," *Proc. Natl. Acad. Sci. USA*, **103**(43), pp. 15739–15746.
- [57] Wong, H.-W., Yelvington, P. E., Timko, M. T., Onasch, T. B., Miake-Lye, R. C., Zhang, J., and Waitz, I. A., 2008, "Microphysical Modeling of Ground-Level Aircraft-Emitted Aerosol Formation: Roles of Sulfur-Containing Species," *J. Propul. Power*, **24**(3), pp. 590–602.
- [58] Jun, M., 2011, "Microphysical Modeling of Ultrafine Hydrocarbon-Containing Aerosols in Aircraft Emissions," Ph.D. dissertation, Department of Aeronautics and Astronautics, Massachusetts Institute of Technology, Cambridge, MA.
- [59] Robinson, A. L., Donahue, N. M., Shrivastava, M. K., Weitkamp, E. A., Sage, A. M., Grieshop, A. P., Lane, T. E., Pierce, J. R., and Pandis, S. N., 2007, "Rethinking Organic Aerosols: Semivolatile Emissions and Photochemical Aging," *Science*, **315**(5816), pp. 1259–1262.
- [60] May, A. A., Presto, A. A., Hennington, C. J., Nguyen, N. T., Gordon, T. D., and Robinson, A. L., 2013, "Gas-Particle Partitioning of Primary Organic Aerosol Emissions: (2) Diesel Vehicles," *Environ. Sci. Technol.*, **47**(15), pp. 8288–8296.
- [61] Lukachko, S. P., Waitz, I. A., Miake-Lye, R. C., and Brown, R. C., 2008, "Engine Design and Operational Impacts on Particulate Matter Precursor Emissions," *ASME J. Eng. Gas Turbines Power*, **130**(2), p. 021505.
- [62] Tremmel, H. G., and Schumann, U., 1999, "Model Simulations of Fuel Sulfur Conversion Efficiencies in an Aircraft Engine: Dependence on Reaction Rate Constants and Initial Species Mixing Ratios," *Aerosp. Sci. Technol.*, **3**(7), pp. 417–430.
- [63] Pande, S. G., and Handy, D. R., 1995, "An In-Depth Evaluation of Combustion Performance Predictors of Aviation Sooting Tendencies," *Energy Fuels*, **9**(3), pp. 448–457.
- [64] Curtis, J., Arnold, F., and Schulte, P., 2002, "Sulfuric Acid Measurements in the Exhaust Plume of a Jet Aircraft in Flight: Implications of the Sulfuric Acid Formation Efficiency," *Geophys. Res. Lett.*, **29**(7), p. 1113.
- [65] Katragkou, E., Wilhelm, S., Arnold, F., and Wilson, C., 2004, "First Gaseous Sulfur (VI) Measurements in the Simulated Internal Flow of an Aircraft Engine During Project PartEmis," *Geophys. Res. Lett.*, **31**, p. L02117.
- [66] Nickels, T. B., and Perry, A. E., 1996, "An Experimental and Theoretical Study of the Turbulent Coflowing Jet," *J. Fluid Mech.*, **309**, pp. 157–182.